scientific reports

OPEN

Synthesis of a magnetic polystyrene-supported Cu(II)-containing heterocyclic complex as a magnetically separable and reusable catalyst for the preparation of *N*-sulfonyl-*N*-aryl tetrazoles

Mahmoud Nasrollahzadeh[1✉], Narjes Motahharifar[1], Khatereh Pakzad[1], Zahra Khorsandi[1,5], Talat Baran[3], Jinghan Wang[4], Benjamin Kruppke[2] & Hossein Ali Khonakdar[2,5]

In this work, a cost-effective, environmentally friendly, and convenient method for synthesizing a novel heterogeneous catalyst via modification of polystyrene using tetrazole-copper magnetic complex [Ps@Tet-Cu(II)@Fe$_3$O$_4$] has been successfully developed. The synthesized complex was analyzed using TEM (transmission electron microscopy), HRTEM (high resolution-transmission electron microscopy), STEM (scanning transmission electron microscopy), FFT (Fast Fourier transform), XRD (X-ray diffraction), FT-IR (Fourier transform-infrared spectroscopy), TG/DTG (Thermogravimetry and differential thermogravimetry), ICP-OES (Inductively coupled plasma-optical emission spectrometry), Vibrating sample magnetometer (VSM), EDS (energy dispersive X-ray spectroscopy), and elemental mapping. *N*-Sulfonyl-*N*-aryl tetrazoles were synthesized in high yields from *N*-sulfonyl-*N*-aryl cyanamides and sodium azide using Ps@Tet-Cu(II)@Fe$_3$O$_4$ nanocatalyst. The Ps@Tet-Cu(II)@Fe$_3$O$_4$ complex can be recycled and reused easily multiple times using an external magnet without significant loss of catalytic activity.

Catalysts have been used widely for chemical transformations; especially organic reactions. However, the effective separation of homogeneous catalysts is a remarkable scientific and engineering challenge. The use of heterogeneous catalysts is an efficient method to solve this problem. Heterogeneous catalysts have many advantages such as easy recovery and recyclability from the reaction media using centrifugation, filtration, and magnetic alteration[1–10]. Heterogeneous catalysts can be immobilized on various supports such as graphene, polymers, magnetic nanoparticles, zeolite, carbon, mesoporous silica, and silica sol–gels[11–26]. In recent decades, polymer-based supports have been studied extensively due to their several specifications, well-controlled structure, and ease of functionalization[15–21]. For example, polystyrene (PS) is one of the extensively used polymers. The introduction of various functions to PS produces effective nanocomposite supports for heterogeneous catalysts[17,20,21].

Nanomaterials are one of the most important types of compounds, which can be applied in different fields[27–37]. Metal nanoparticles (MNPs) are the most important nanomaterials[38–45]. MNPs have most of the particular features of an appropriate catalyst, including low price, great activity, high surface area, low toxicity, significant thermal stability, simple recoverability, and excellent recyclability[46–56]. From this perspective, MNPs-supported

[1]Department of Chemistry, Faculty of Science, University of Qom, PO Box 37185-359, Qom, Iran. [2]Max Bergmann Center of Biomaterials, Institute of Materials Science, Technische Universität Dresden, 01069 Dresden, Germany. [3]Department of Chemistry, Faculty of Science and Letters, Aksaray University, 68100 Aksaray, Turkey. [4]Department of Materials Science and Engineering, Research Institute of Advanced Materials, Seoul National University, Seoul 08826, Republic of Korea. [5]Department of Processing, Iran Polymer and Petrochemical Institute, Tehran, Iran. ✉email: mahmoudnasr81@gmail.com; m.nasrollahzadeh@qom.ac.ir

catalysts are associated with green chemistry and sustainability[57–65]. Among various MNPs, copper-based catalysts represent considerable catalytic activities. Copper has received wide attention as an effective transition metal owing to its remarkable advantages such as numerous sources, low cost, diversity, low environmental hazards, and extensive applications[66–72]. In recent years, scientists have tried to decrease the costs of organic reactions by replacing palladium with cheap metals such as copper[73–75].

Today, researchers are paying a lot of attention to the field of catalysis[76–82]. Recently, magnetic NPs have been widely used as catalyst supports for different organic transformations[13,18,20,57]. The most important features of magnetic nanocatalysts include their high surface-to-volume ratio, which leads to high catalytic activities, high dispersion, and excellent stability. Moreover, these catalysts contain the green advantage of suitable and efficient recyclability, owing to their simplicity of separation using a magnet. Catalysts supported on super magnetic NPs have successfully catalyzed various organic reactions[58,59]. Among heterogeneous catalysts, magnetite/polymer nanocomposite is one of the most effective nanocomposites. Fe_3O_4 NPs dispersed on polymer surfaces are superparamagnetic catalysts in various chemical reactions[17].

Tetrazole is an important synthetic compound with wide applications in various fields such as pharmacology, biochemistry, medicinal chemistry, photography, and imaging chemicals. In fact, various tetrazoles; especially 5-substituted 1H-tetrazoles and aminotetrazoles have been applied to synthesize biologically active compounds in recent years[13,83–85]. The [2 + 3] cycloaddition reaction is a conventional method for the synthesis of tetrazoles. Given the medicinal applications of tetrazoles, different synthetic methodologies have been widely developed for their synthesis.[13,66,67,85]

Among tetrazoles, aminotetrazoles have received much attention because of their wide-ranging applications. However, the lack of convenient methods for the synthesis of these compounds or their derivatives such as N-sulfonyl-N-aryl tetrazoles strongly restricts their potential medical applications[66,67,85]. Thus, it is desirable to develop a convenient and efficient method for the synthesis of N-sulfonyl-N-aryl tetrazoles.

Following our research on the progress of modern catalytic systems, in this study, copper NPs immobilized on magnetic tetrazole-functionalized polystyrene [Ps@Tet-Cu(II)@Fe₃O₄] have been investigated as a highly effective catalyst (Scheme 1). After the characterization of the synthesized complex by various techniques, the catalytic activity of the complex in the synthesis of N-sulfonyl-N-aryl tetrazoles was studied (Scheme 2).

Experimental

Instruments and reagents.
TEM, STEM, and NMR spectra were recorded on JEM-F200 JEOL, JEM-F200-TFEG-JEOL Ltd, and Bruker Avance DRX 600 MHz instruments, respectively. The FT-IR spectra and XRD patterns of the samples were obtained using a Perkin Elmer 100 spectrophotometer and a Philips model PW 1373 diffractometer, respectively. The elemental compositions of the synthesized nanoparticle were determined by EDS coupled with Map. STA 1500 Rheometric-Scientific conducted TGA measurements under N_2 flow. VSM analysis was performed using a magnetometer at 298 K (LBKFB).
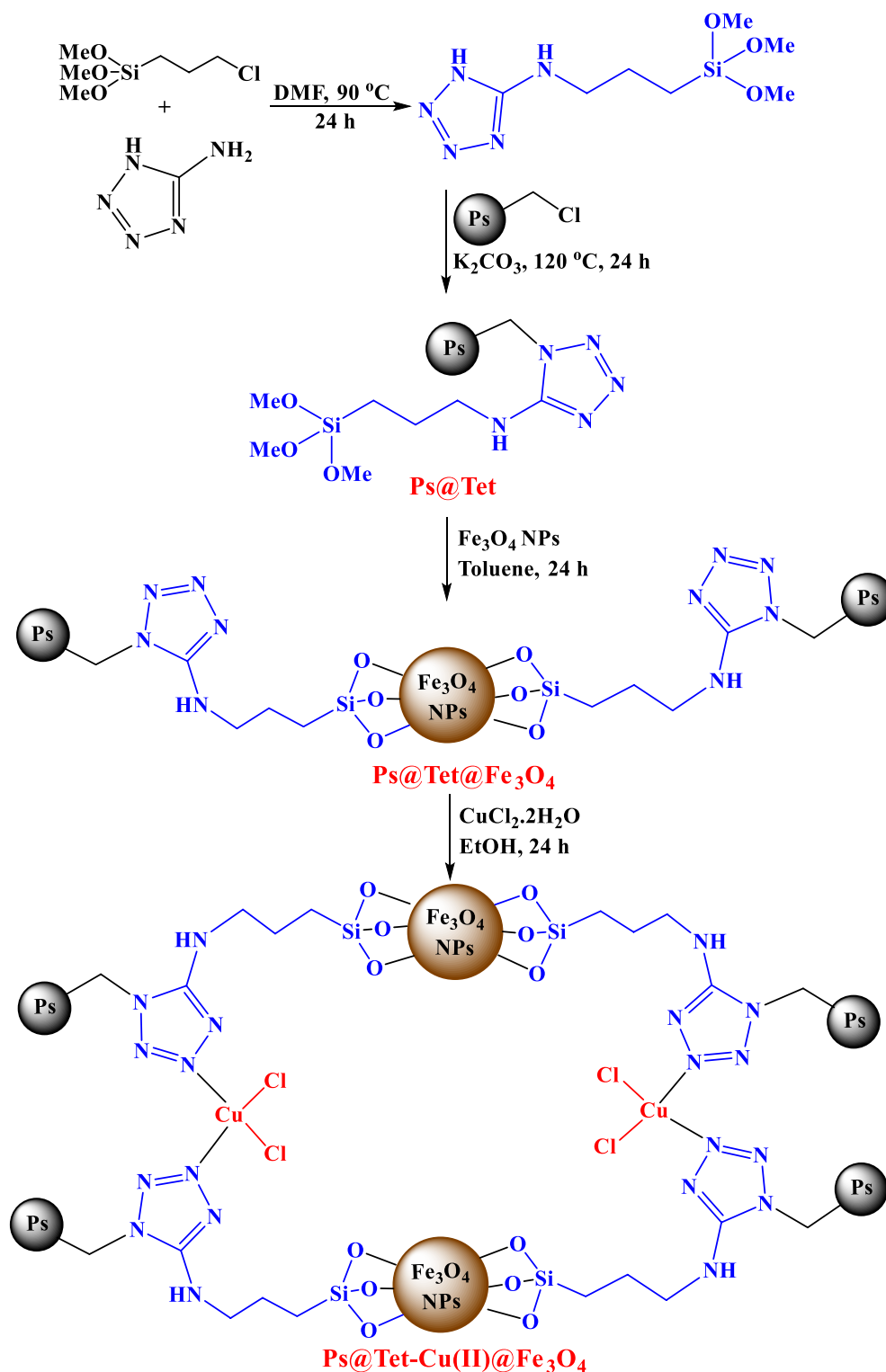
Synthesis of Ps@Tet-Cu(II)@Fe₃O₄.
In a 250 mL beaker, a solution of 5-amino-1H-tetrazole (5 mmol), TMOS [(3-chloropropyl)trimethoxysilane] (5 mmol) in DMF (60 mL) solvent was stirred for 24 h at 90 ℃. Chloromethylated polystyrene (2 g) and potassium carbonate (5 mmol) were then added to the reaction media, which was stirred for another 24 h at 120 ℃. After cooling the reaction mixture, the obtained Ps@Tet was filtrated, washed with DMF, and dried at 70 °C. Afterward, 1 g of Ps@Tet, 1.5 g of Fe₃O₄ NPs, and 50 mL of toluene were mixed vigorously under reflux conditions for 24 h. The synthesized Ps@Tet@Fe₃O₄ was then separated using an external magnet, washed with toluene, and dried at 70 °C. In the next step, 1 g of the obtained Ps@Tet@Fe₃O₄ and 0.5 g of CuCl₂.6H₂O were mixed constantly in 50 mL of ethanol solvent at 85 °C for one day. Upon completion of the reaction, the synthesized magnetic complex Ps@Tet-Cu(II)@Fe₃O₄ was separated using a magnet, washed with EtOH, and dried at 70 °C (Scheme 1).

General process for the synthesis of N-sulfonyl-N-aryl tetrazoles.
In a 50 mL beaker, N-sulfonyl-N-aryl cyanamide (1 mmol), NaN₃ (1.5 mmol), and Ps@Tet-Cu(II)@Fe₃O₄ (0.05 g) catalyst were continuously mixed in DMF (10 mL) solvent at 120 ℃. The progress of the reaction was followed by TLC. After completion of the reaction, the magnetic catalyst was separated by an external magnet. Afterward, 25 mL of hydrochloric acid (2 N) and 25 mL of ethyl acetate were added to the reaction mixture, which was then stirred vigorously. After the separation of the organic phase, the aqueous phase was extracted by ethyl acetate (25 mL) three times and the organic layer was concentrated. The product was then purified by recrystallization from ethanol. All products were identified by NMR and FT-IR spectroscopy[66,67,85].

Characterization data of new product.
4-Bromo-N-(3-bromophenyl)-N-(1H-tetrazol-5-yl)benzenesulfonamide. FT-IR (KBr, cm⁻¹) 3445, 3137, 1632, 1576, 1468, 1398, 1364, 1232, 1171, 966, 813, 818, 747, 690, 608, 577, 548, 502; ¹H NMR (600 MHz, DMSO-d_6) δ_H = 7.83 (d, J = 8.6 Hz, 2H), 7.73 (d, J = 8.6 Hz, 2H), 7.50 (d, J = 8.0 Hz, 1H), 7.36 (s, 1H), 7.30 (t, J = 8.0 Hz, 1H), 7.22 (d, J = 8.0 Hz, 1H); ¹³C NMR (150 MHz, DMSO-d_6) δ_C = 159.2, 140.5, 137.1, 132.1, 131.0, 130.6, 130.1, 129.8, 127.7, 126.2, 121.2; Anal. Calcd for $C_{13}H_9Br_2N_5O_2S$: C, 34.01; H, 1.98; N, 15.25. Found: C, 34.13; H, 2.12; N, 15.37.
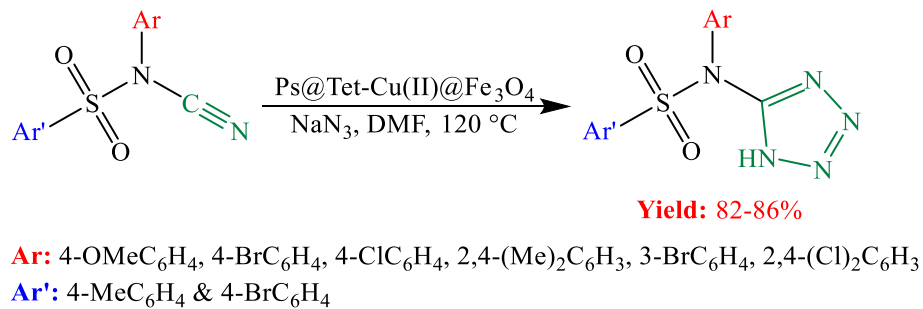
Result and discussion

Characterization of Ps@Tet-Cu(II)@Fe₃O₄.
The XRD patterns of the synthesized Ps@Tet@Fe₃O₄ and Ps@Tet-Cu(II)@Fe₃O₄ complex are illustrated in Fig. 1. The XRD patterns demonstrate the presence of Fe₃O₄ NPs with diffraction angles of 30.2°, 35.8°, 43.5°, 53.7°, 57.2°, and 62.8°, which are assigned to the crystal planes of (220), (311), (400), (511), (440), and (533), respectively[67].

Scheme 1. Synthesis of Ps@Tet-Cu(II)@Fe$_3$O$_4$.

FT-IR analysis was applied to confirm the presence of functional groups in complex interactions. The FT-IR spectra of the synthesized Ps@Tet, Ps@Tet@Fe$_3$O$_4$ and Ps@Tet-Cu(II)@Fe$_3$O$_4$ complex are illustrated in Fig. 2. The peaks at around 1153 cm^{-1}, 1492 cm^{-1}, 1650 cm^{-1}, and 2922 cm^{-1} correspond to Si–O, N=N, C=N, and C–H (sp^3) stretching vibrations, respectively. In addition, the peaks at 550 cm^{-1} and 3300–3450 cm^{-1} are due to the Fe–O bond stretching and O–H functional groups of Fe$_3$O$_4$, respectively[67].

The TEM analysis of Ps@Tet, Ps@Tet@Fe$_3$O$_4$ and Ps@Tet-Cu(II)@Fe$_3$O$_4$ was applied to confirm the formation of Cu NPs on the surface of Ps@Tet@Fe$_3$O$_4$ (Figs. 3, 4, 5). As observed in Figs. 3, 4, 5, Cu NPs have been

Ar: 4-OMeC$_6$H$_4$, 4-BrC$_6$H$_4$, 4-ClC$_6$H$_4$, 2,4-(Me)$_2$C$_6$H$_3$, 3-BrC$_6$H$_4$, 2,4-(Cl)$_2$C$_6$H$_3$
Ar': 4-MeC$_6$H$_4$ & 4-BrC$_6$H$_4$

Scheme 2. Synthesis of *N*-sulfonyl-*N*-aryl tetrazoles.
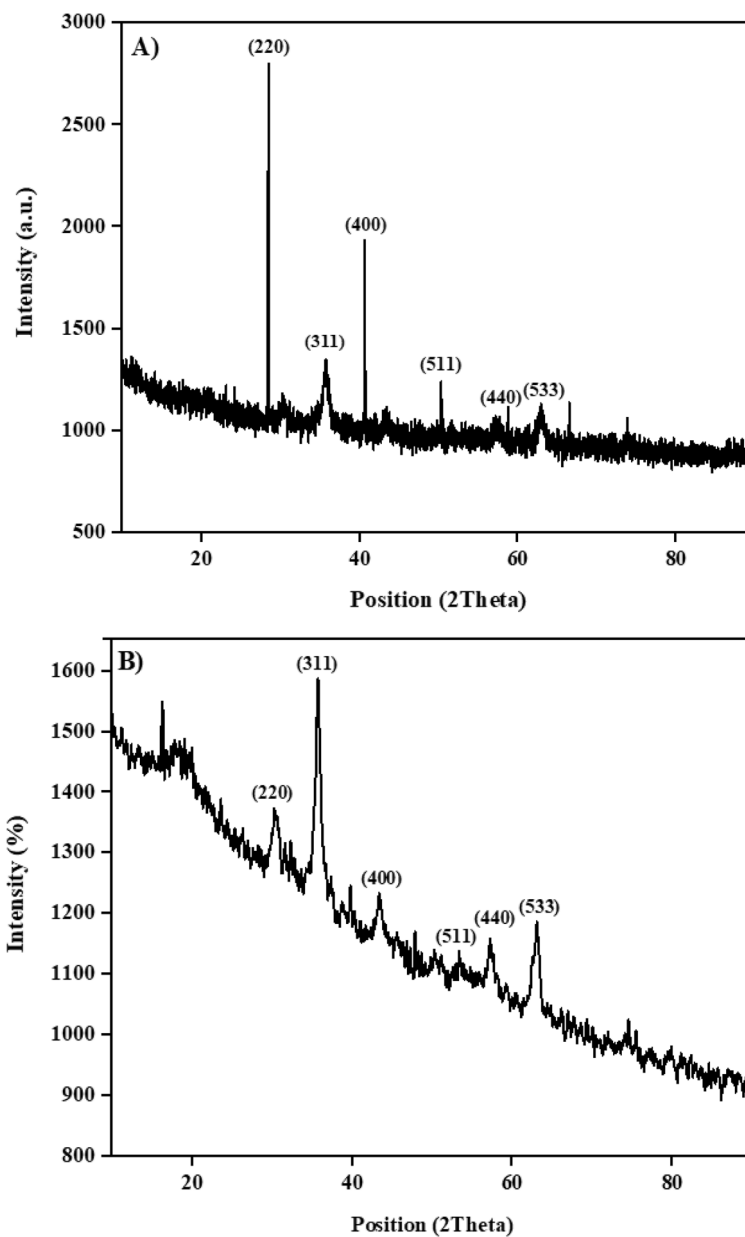
Figure 1. XRD powder pattern of Ps@Tet@Fe$_3$O$_4$ (**A**) and Ps@Tet-Cu(II)@Fe$_3$O$_4$ (**B**).
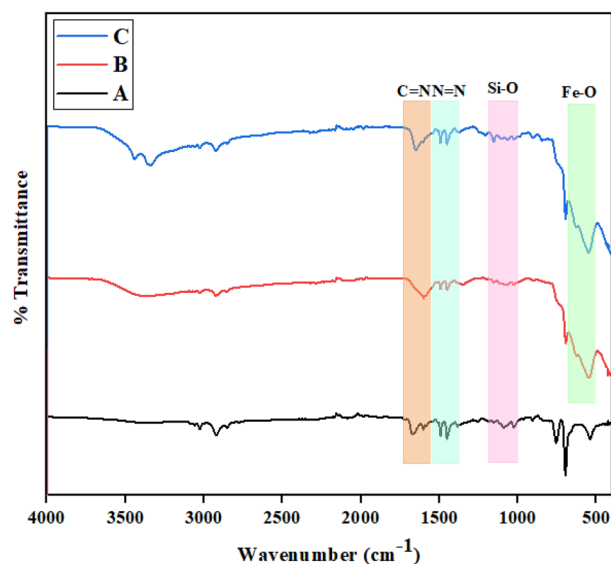
Figure 2. FT-IR spectra of Ps@Tet (**A**), Ps@Tet@Fe$_3$O$_4$ (**B**) and Ps@Tet-Cu(II)@Fe$_3$O$_4$ (**C**).

successfully loaded on the Ps@Tet@Fe$_3$O$_4$. The TEM and HRTEM images illustrate the fine dispersion of Cu NPs with the size of 8–10 nm on the Ps@Tet@Fe$_3$O$_4$ surface, accumulated in sites corresponding to iron oxide NPs. The HRTEM and FFT images of the Ps@Tet-Cu(II)@Fe$_3$O$_4$ show that the nanoparticles are highly crystalline. The STEM image confirms a homogeneously assembled nanostructured catalyst (Figs. 4 and 5).

The EDS spectroscopy was used to determine the composition of Ps@Tet@Fe$_3$O$_4$ and Ps@Tet-Cu(II)@Fe$_3$O$_4$ complex (Fig. 6). The EDS analysis shows the presence of desired elements in their chemical structure. Figure 6 confirms that C, O, Si, and Fe are the main components present in both Ps@Tet@Fe$_3$O$_4$ and Ps@Tet-Cu(II)@Fe$_3$O$_4$ along with Cu and Cl elements, which are present only in the Ps@Tet-Cu(II)@Fe$_3$O$_4$ complex, further reaffirming the formation of the final catalyst. The amount of Cu incorporated into the Ps@Tet-Cu(II)@Fe$_3$O$_4$ complex was found to be 19.7 w%, as measured by EDS. According to ICP-OES analysis, the amount of Cu is 7.6 wt.%.

Elemental mapping of Ps@Tet, Ps@Tet@Fe$_3$O$_4$, and Ps@Tet-Cu(II)@Fe$_3$O$_4$ are presented in Figs. 7, 8, 9. Elemental mapping was performed to determine the distribution of the elements on Ps@Tet-Cu(II)@Fe$_3$O$_4$ complex surface. Figures 7, 8, 9 confirm that C, O, Si, and N are main components present in Ps@Tet, Ps@Tet@Fe$_3$O$_4$, and Ps@Tet-Cu(II)@Fe$_3$O$_4$, along with Fe element, which was present only in the Ps@Tet@Fe$_3$O$_4$ and Ps@Tet-Cu(II)@Fe$_3$O$_4$ (Figs. 8 and 9). Additionally, the presence of Cl and Cu was determined using elemental mapping (Fig. 9); which indicated the uniform dispersion of Cu on the Ps@Tet@Fe$_3$O$_4$ surface.

The magnetic properties of the synthesized Ps@Tet-Cu(II)@Fe$_3$O$_4$ complex were studied using VSM, as shown in Fig. 10. The specific saturation magnetization values (Ms) were calculated to be 60 and 20 emu/g for Fe$_3$O$_4$ NPs and Ps@Tet-Cu(II)@Fe$_3$O$_4$ complex, respectively, indicating that the modification of the surface and the addition of portions have led to decreased saturation magnetizations. Therefore, this complex has superparamagnetic characteristics and high magnetization values, enabling its separation by an external magnet from the reaction mixture.
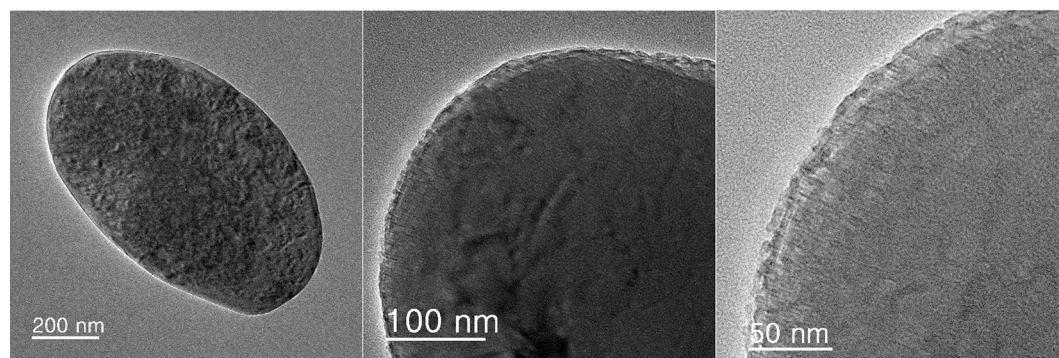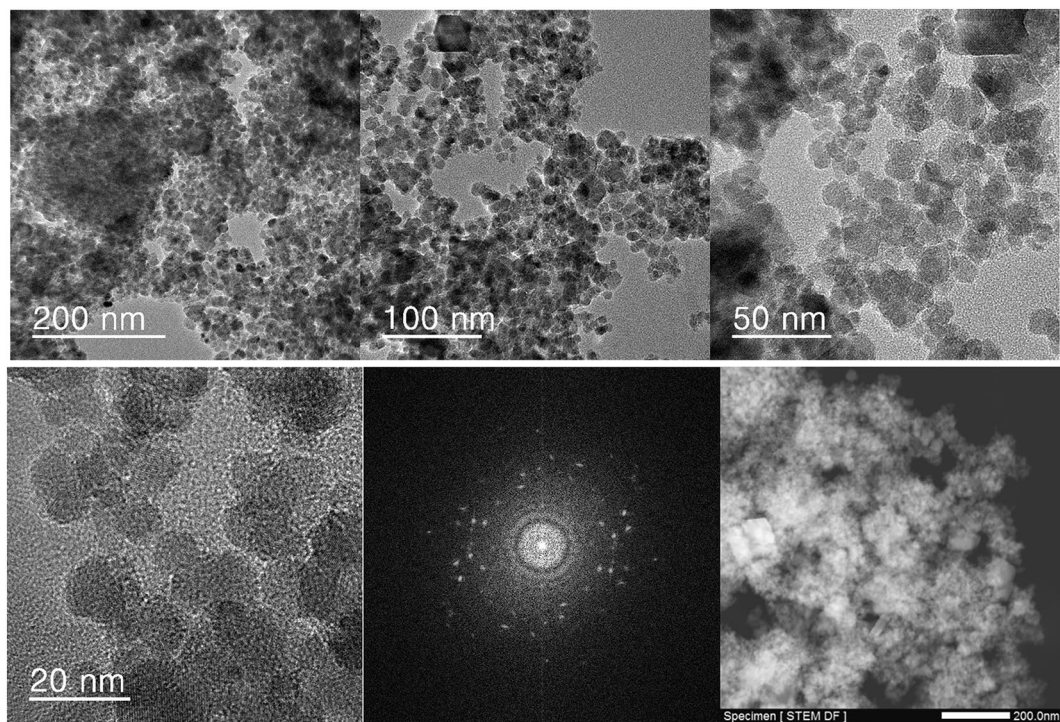

Figure 3. TEM images of Ps@Tet.

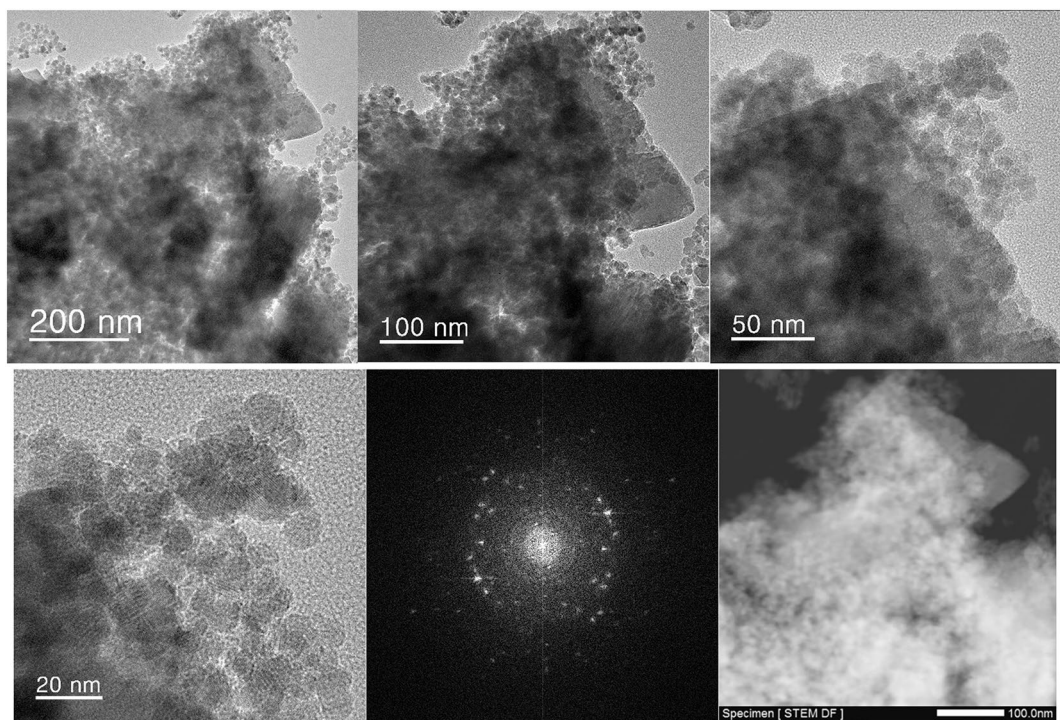**Figure 4.** TEM, HRTEM, FFT and STEM images of Ps@Tet@Fe$_3$O$_4$.

Figure 5. TEM, HRTEM, FFT and STEM images of Ps@Tet-Cu(II)@Fe$_3$O$_4$.

The TG/DTG analysis is a great technique to measure thermal stability. Therefore, the thermal stability of the synthesized complex was checked over a temperature range of 30–700 ℃ (Fig. 11). The polymer-supported Cu(II) complex is stable up to 300 ℃. The first step of degradation (up to 300 ℃) is due to the removal of water and organic solvents. The second mass reduction is related to the degradation of organic groups such as 5-amino-1H-tetrazole in the temperature range of 300–410 ℃. The final degradation stage corresponds to the complete
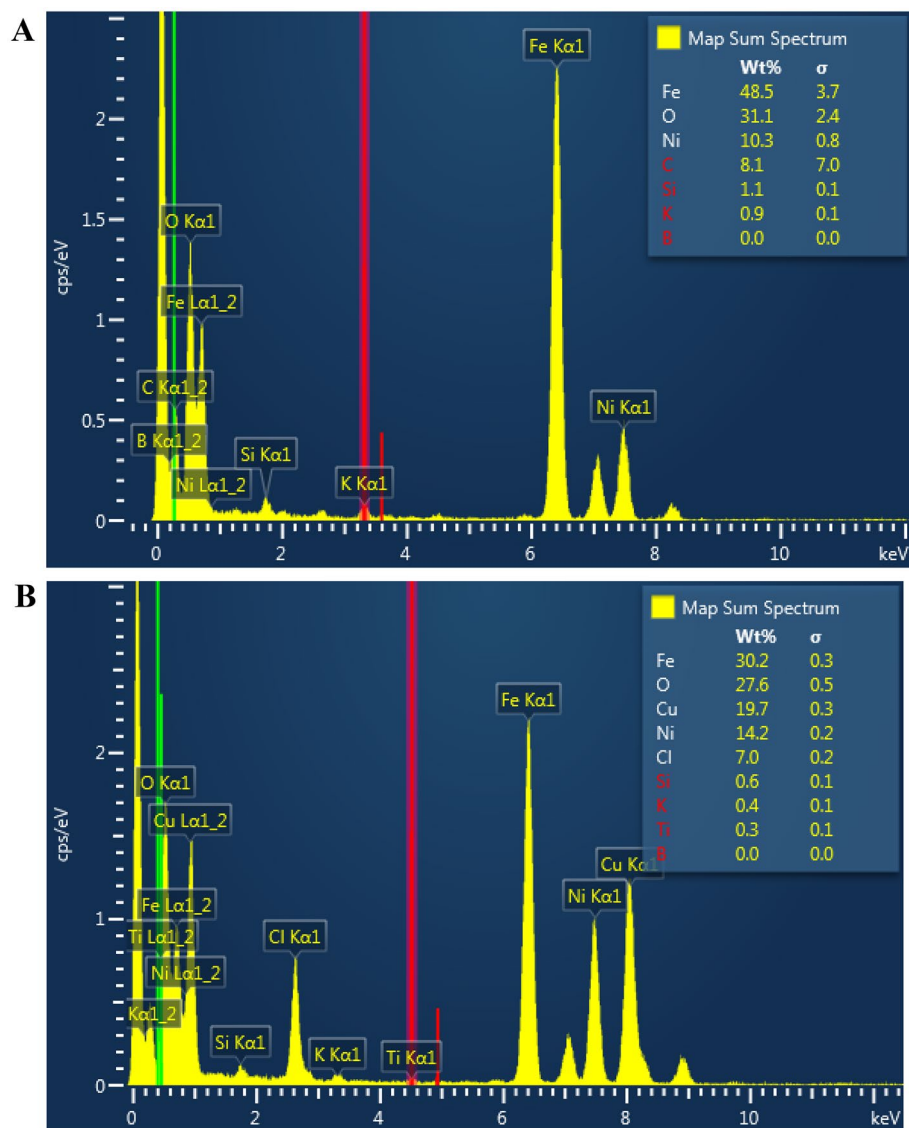
Figure 6. EDS spectra of Ps@Tet@Fe$_3$O$_4$ (**A**) and Ps@Tet-Cu(II)@Fe$_3$O$_4$ (**B**).

decomposition of functional groups of the catalyst. This degradation occurs when the temperature increases from 500 to 600 °C.

Synthesis of *N*-sulfonyl-*N*-aryl tetrazoles. The catalytic performance of Ps@Tet-Cu(II)@Fe$_3$O$_4$ was investigated in the [2 + 3] cycloaddition reaction. The synthesis of *N*-sulfonyl-*N*-aryl tetrazoles by the reaction of *N*-sulfonyl-*N*-aryl cyanamide and NaN$_3$ as a model reaction in the presence of Ps@Tet-Cu(II)@Fe$_3$O$_4$ complex as a novel catalyst was studied for this purpose.

In the first step, the optimization of the reaction conditions was performed using *N*-(4-chlorophenyl)-*N*-cyano-4-methylbenzenesulfonamide (1 mmol) as a model substrate, NaN$_3$ (1.5 mmol), Ps@Tet-Cu(II)@Fe$_3$O$_4$ complex and DMF solvent at 120 °C. The results of the optimization reactions are shown in Table 1. As observed, the reaction does not proceed in the absence of the catalyst.

After the optimization of the reaction, the efficiency of Ps@Tet-Cu(II)@Fe$_3$O$_4$ complex for the synthesis of various derivatives of *N*-sulfonyl-*N*-aryl tetrazole using various types of *N*-sulfonyl-*N*-aryl cyanamides containing electron-withdrawing as well as electron-donating groups was investigated (Table 2). Both groups on the aromatic ring of *N*-sulfonyl-*N*-aryl cyanamides favor the formation of the resulting target tetrazoles in high yields and short reaction times.

The proposed mechanism for the synthesis of tetrazoles using Ps@Tet-Cu(II)@Fe$_3$O$_4$ complex is presented in Scheme 3. According to the reaction procedure, initially, an interaction occurs between the CN group of *N*-sulfonyl-*N*-aryl cyanamides in the presence of Ps@Tet-Cu(II)@Fe$_3$O$_4$ complex. Next, N$_3^-$ addition to the activated CN group gives the intermediate (**A**). Finally, the intramolecular cyclization of (**A**) leads to the desired product. This method has merits including high yields, short reaction time, and lack of production of HN$_3$ toxic gas[85].
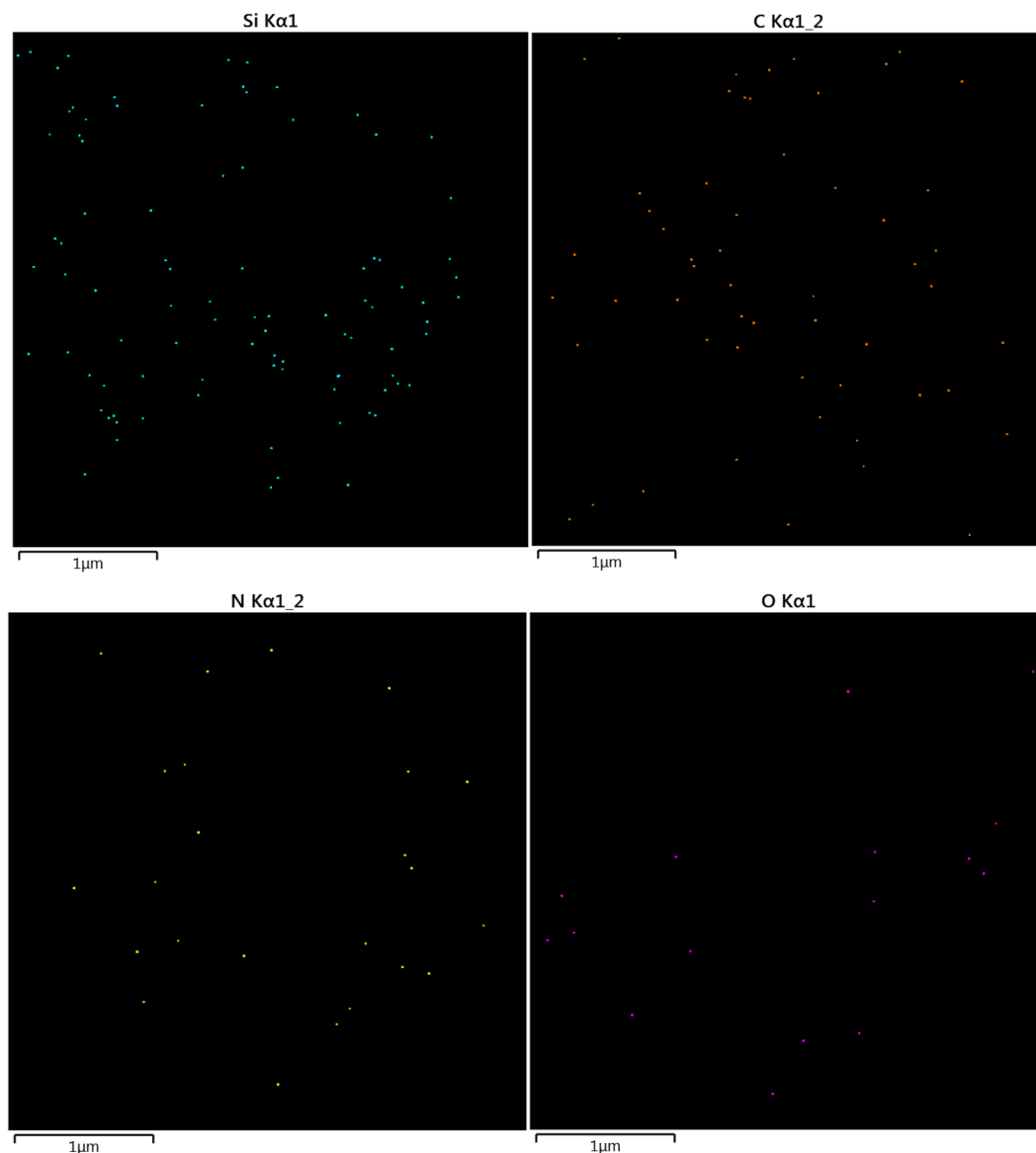
Figure 7. Elemental mapping of Ps@Tet.

Summary and discussion.   *N*-Sulfonyl-*N*-aryl tetrazole derivatives are very new compounds synthesized and reported by our research groups in recent years. In two previous publications, the synthesis of these novel derivatives through different reaction conditions have been reported. For example, for the first time, the synthesis of *N*-sulfonyl-*N*-aryl tetrazole derivatives was carried out in the presence of NaN_3, $ZnBr_2$, and H_2O under reflux conditions for 24 h[85]. Although the product yields were relatively good, the reaction time was very long. In another study, the synthesis of these derivatives using Cu NPs@Fe_3O_4-chitosan catalyst, NaN_3, and H_2O under reflux conditions was investigated[66]. The drawback of the latter synthesis procedure was still the long reaction time (22 h). In addition, in our recent study, the synthesis of *N*-sulfonyl-*N*-aryl tetrazole derivatives using magnetic chitosan functionalized trichlorotriazine-5-amino-1*H*-tetrazole copper(II) complex catalyst and DMF solvent under reflux conditions has been reported[67]. The reaction suffered from long reaction time (40 min). Nevertheless, in the present work, *N*-sulfonyl-*N*-aryl tetrazole derivatives have been synthesized with high efficiency (82–86%) and in very short reaction times (25–35 min).
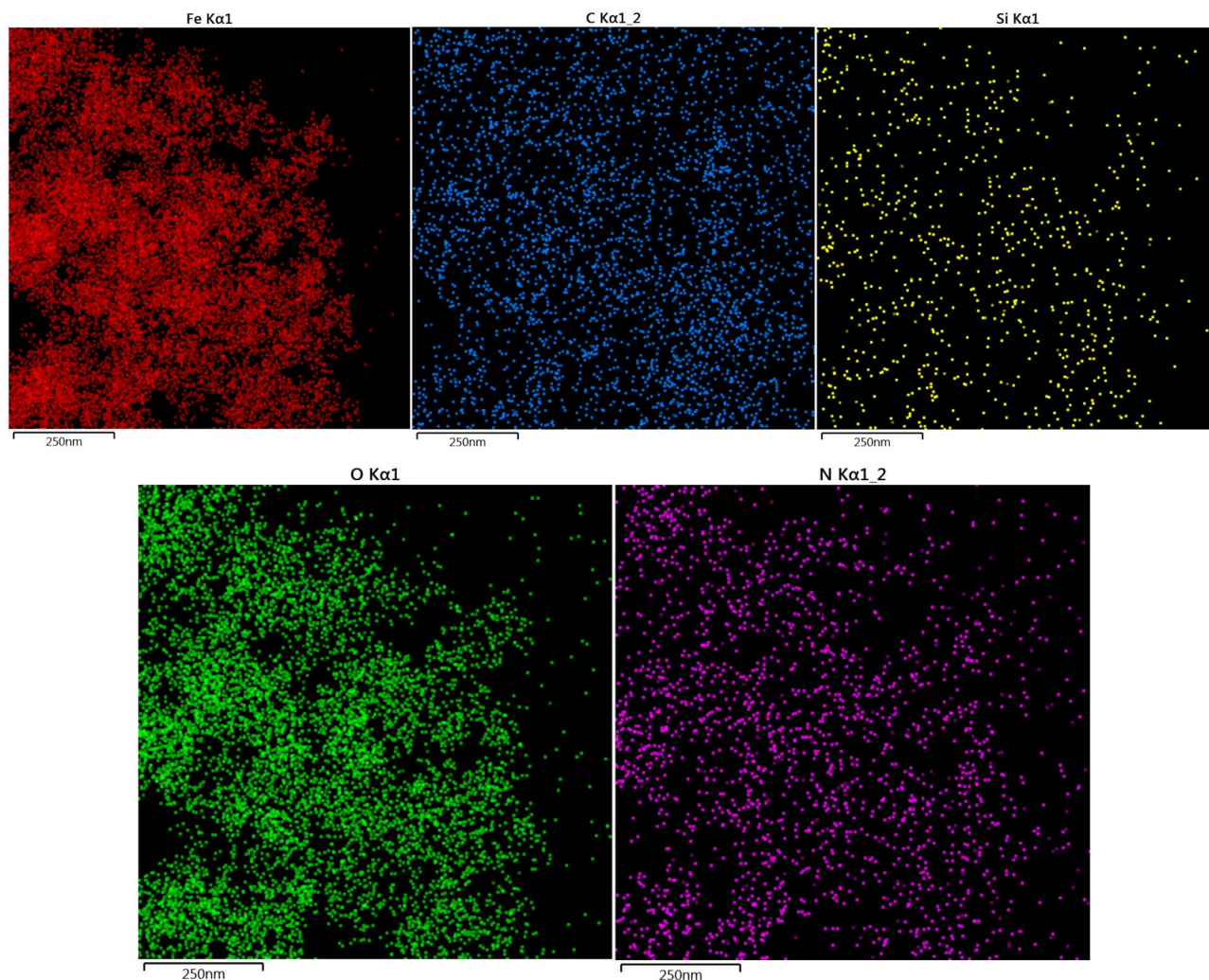
Figure 8. Elemental mapping of Ps@Tet@Fe$_3$O$_4$.

Catalyst recyclability. Reusability of heterogeneous catalysts is the most important advantage for practical purposes; especially for industrial applications. After completing the reaction, this magnetic complex was separated easily from the reaction media by an external magnet, washed with ethanol, dried, and reused for the same reaction without any significant reduction in the desired yields. Ps@Tet-Cu(II)@Fe$_3$O$_4$ exhibited a high activity over five runs, which confirms the catalyst stability. After the last run, the characterization of the recovered catalyst by TEM analysis (Fig. 12) showed a stable morphology and relatively dispersed NPs even after five runs as well as the stable structure of the recycled catalyst. To check the heterogeneity of Ps@Tet-Cu(II)@Fe$_3$O$_4$ catalyst, the filtrate of each cycle was analyzed by ICP-OES analysis. It was shown that less than 0.1% of the total amount of the original copper species was lost in the solution during a reaction.

Conclusions

A novel, easily recoverable, and suitable heterogeneous catalyst has been developed for the synthesis of *N*-sulfonyl-*N*-aryl tetrazole derivatives. The significant advantages of Ps@Tet-Cu(II)@Fe$_3$O$_4$ complex as a magnetic nanocatalyst are its high surface area, simple separation, and outstanding stability. Afterward, the morphology and structure of the synthesized complex were investigated using TEM, HRTEM, STEM, FFT, XRD, FT-IR, TG/DTG, VSM, EDS, and elemental mapping. The catalytic activity of the obtained complex for the synthesis of *N*-sulfonyl-*N*-aryl tetrazole derivatives was checked. The advantages of the method include easy work-up, high yields, and avoidance of the use of harmful and hazardous hydrazoic acid. The magnetic nanocatalyst is environmentally friendly and commercial because it can be recovered using an external magnet and reused in the same reaction without considerable loss of catalytic activity.
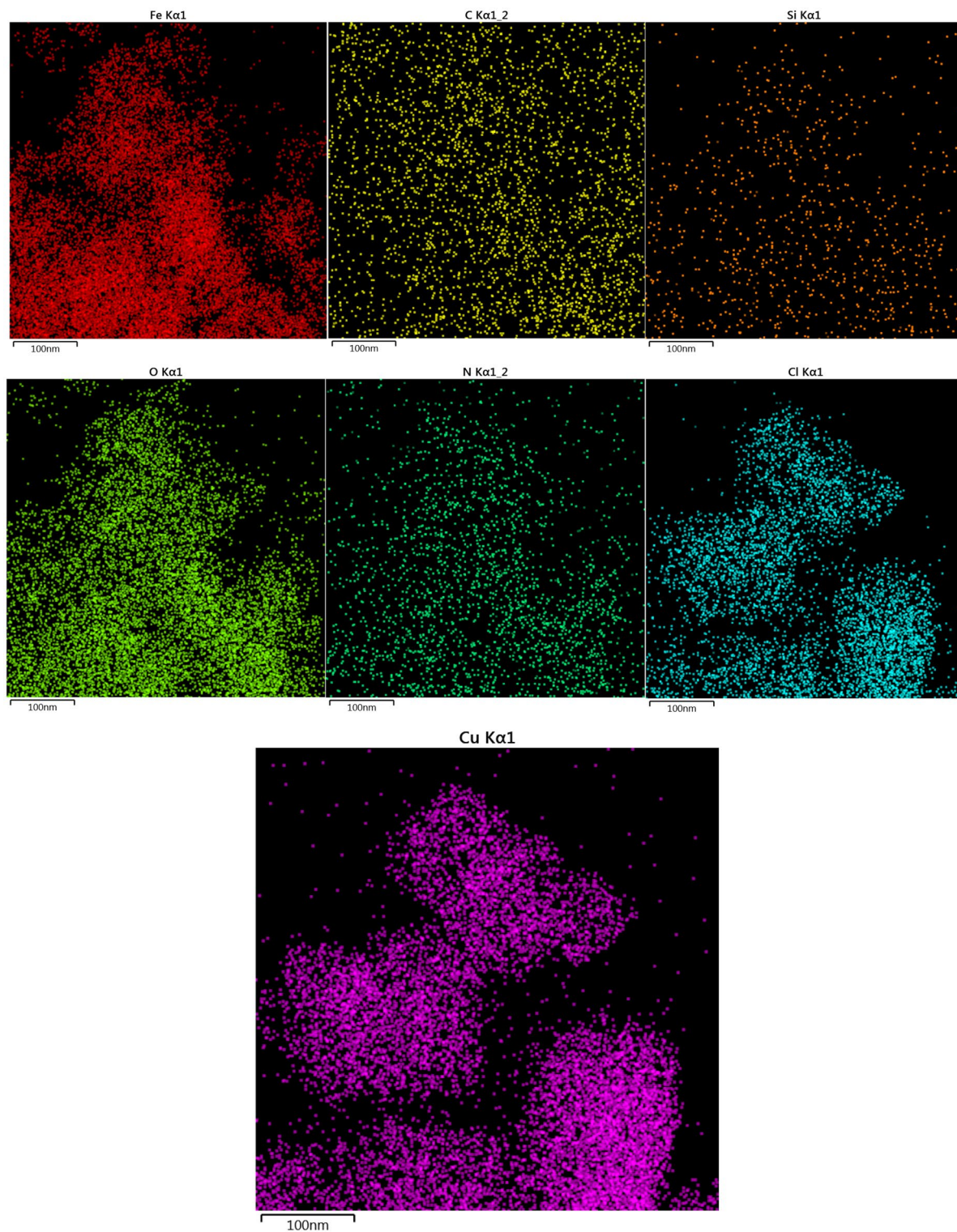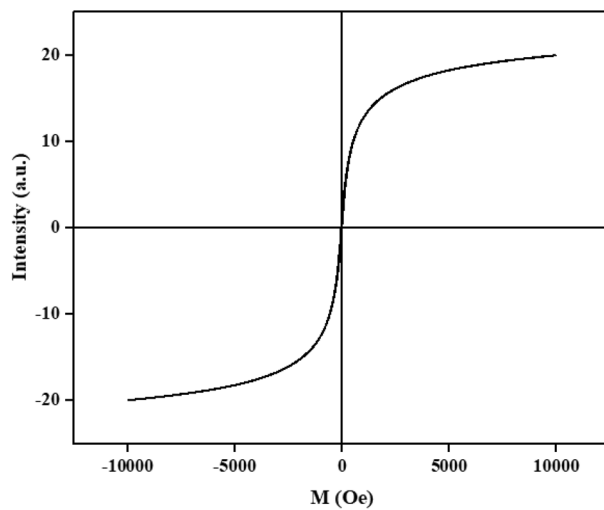
Figure 9. Elemental mapping of Ps@Tet-Cu(II)@Fe$_3$O$_4$.
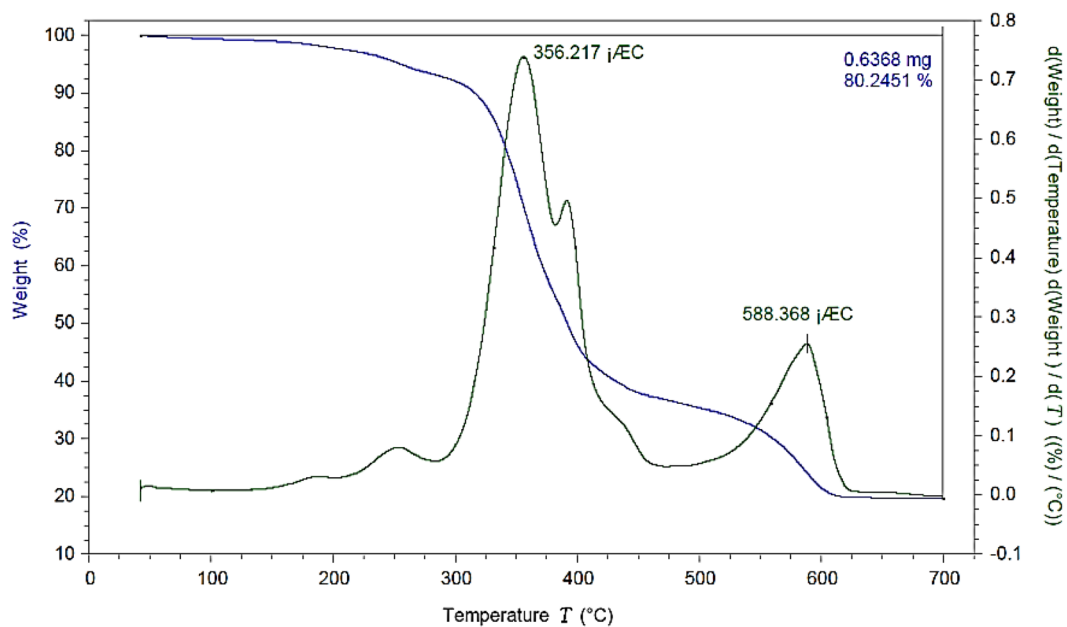
Figure 10. VSM analysis of Ps@Tet-Cu(II)@Fe$_3$O$_4$.
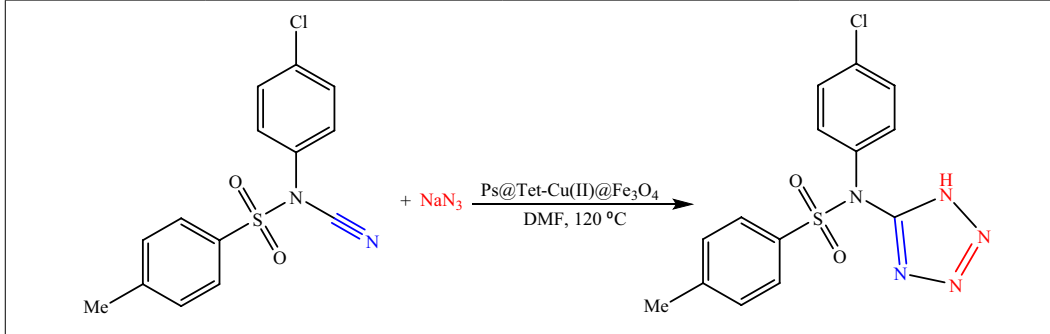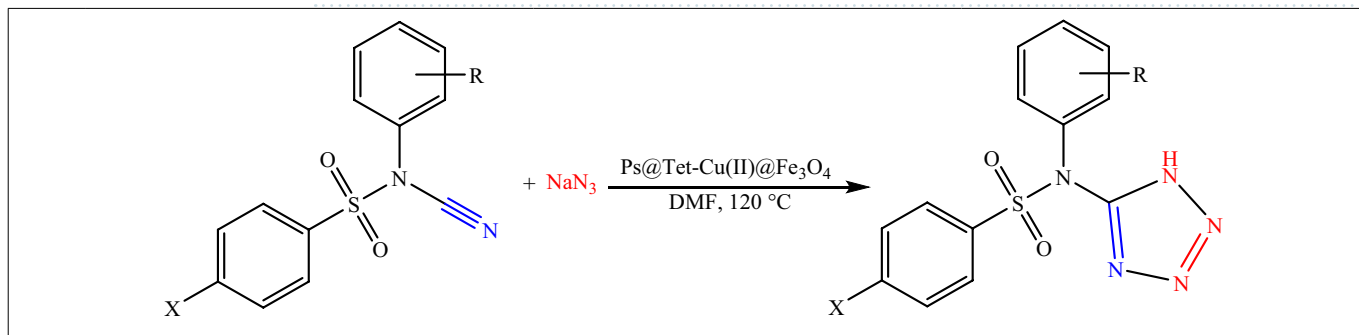
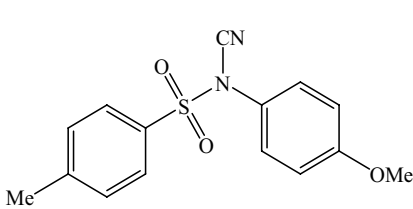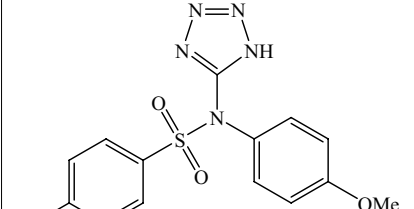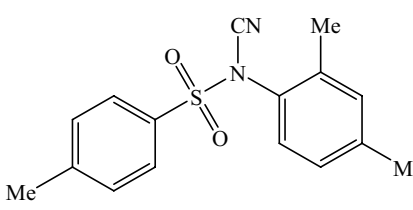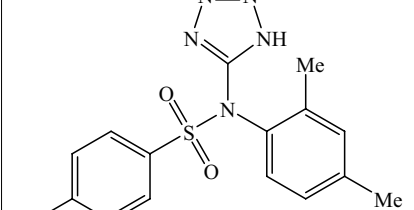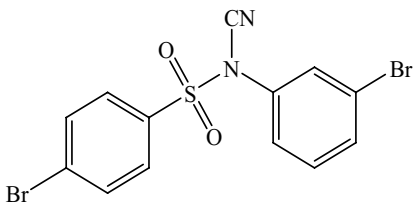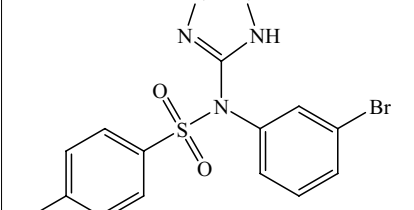**Figure 11.** TG/DTG analysis of Ps@Tet-Cu(II)@Fe$_3$O$_4$.

Entry	Catalyst (g)	Time (min)	Yield[b] (%)
1	0	100	0
2	0.01	65	69
3	0.03	45	78
4	0.05	25	86
5	0.07	25	86

Table 1. Optimization of reaction conditions[a]. [a] Reaction conditions: *N*-(4-chlorophenyl)-*N*-cyano-4-methylbenzenesulfonamide (1 mmol), NaN$_3$ (1.5 mmol), Ps@Tet-Cu(II)@Fe$_3$O$_4$, DMF (10 mL), 120 ℃. [b] Isolated yield.

Entry	Initial substance	Product	Time (min)	Yield[b] (%)	TON	TOF (min^{-1})
1			25	86	14,405	576
2			30	85	14,237	474
3			30	82	13,735	458
Continued						

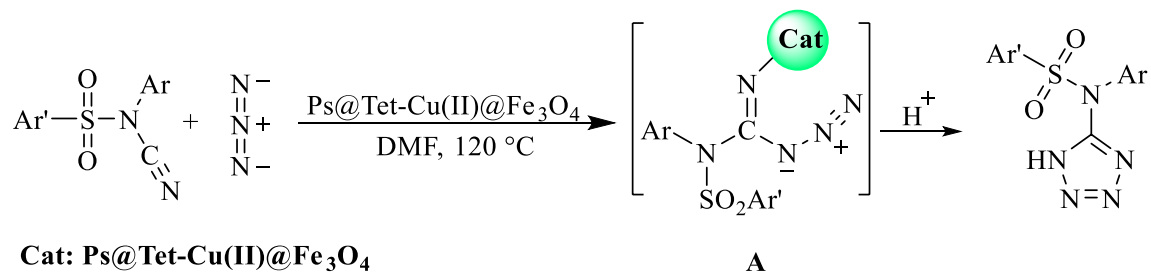| Entry	Initial substance	Product	Time (min)	Yield[b] (%)	TON	TOF (min⁻¹)
4			30	84	14,070	469
5			35	82	13,735	392
6			30	83	13,902	463
7			30	86	14,405	480
8			30	84	14,070	469

Table 2. Synthesis of tetrazoles using Ps@Tet-Cu(II)@Fe₃O₄ complex.[a] [a]Reaction conditions: *N*-sulfonyl-*N*-aryl cyanamide (1 mmol), NaN₃ (1.5 mmol), Ps@Tet-Cu(II)@Fe₃O₄ (0.05 g), DMF (10 mL), 120 ℃. [b] Isolated yield.

Cat: Ps@Tet-Cu(II)@Fe₃O₄

A

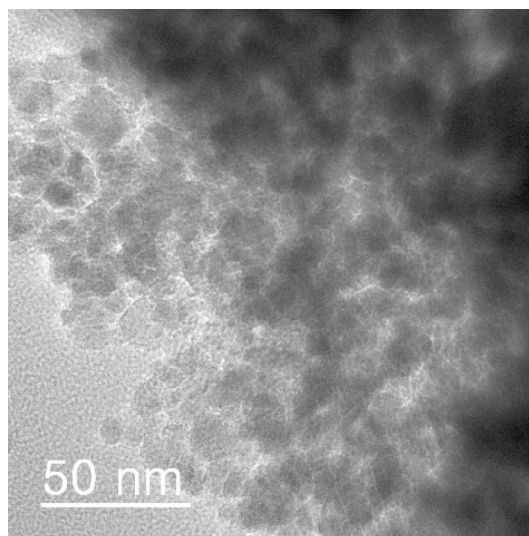**Scheme 3.** Proposed mechanism for the synthesis of tetrazoles.

Figure 12. TEM image of the recycled Ps@Tet-Cu(II)@Fe₃O₄.

Data availability
The datasets used and/or analyzed during the current study are available from the corresponding author on reasonable request.

References
1. Polshettiwar, V. & Varma, R. S. Nanoparticle-supported and magnetically recoverable ruthenium hydroxide catalyst: Efficient hydration of nitriles to amides in aqueous medium. *Chem. Eur. J.* **15**(7), 1582–1586 (2009).
2. Miao, C. X., He, L. N., Wang, J. Q. & Gao, J. Biomimetic oxidation of alcohols catalyzed by TEMPO-functionalized polyethylene glycol and copper(I) chloride in compressed carbon dioxide. *Synlett* **20**(20), 3291–3294 (2009).
3. Jayakumar, M. *et al.* Heterogeneous base catalysts: Synthesis and application for biodiesel production—A review. *Bioresour. Technol.* **331**, 125054 (2021).
4. Appaturi, J. N. *et al.* A review of the recent progress on heterogeneous catalysts for Knoevenagel condensation. *Dalton Trans.* **50**, 4445–4469 (2021).
5. Liu, P., Li, S., Zhang, L., Yin, X. & Ma, Y. Shearing bridge bonds in carbon nitride vesicles with enhanced hot carrier utilization for photocatalytic hydrogen production. *Catal. Sci. Technol.* **12**, 4193–4200 (2022).
6. Huang, Z. *et al.* Highly efficient oxidation of propane at low temperature over a Pt-Based catalyst by optimization support. *Environ. Sci. Technol.* **56**(23), 17278–17287 (2022).
7. Zhang, K.-Q. *et al.* Multifunctional Ag(I)/CAAA-amidphos complex-catalyzed asymmetric [3 + 2] cycloaddition of α-substituted acrylamides. *ACS Catal.* **11**(9), 5100–5107 (2021).
8. Huang, Z. *et al.* Total oxidation of light alkane over phosphate-modified Pt/CeO₂ catalysts. *Environ. Sci. Technol.* **56**(13), 9661–9671 (2022).
9. Liu, J. *et al.* High-yield aqueous synthesis of partial-oxidized black phosphorus as layered nanodot photocatalysts for efficient visible-light driven degradation of emerging organic contaminants. *J. Clean. Prod.* **377**, 134228 (2022).
10. Huo, J., Wei, H., Fu, L., Zhao, C. & He, C. Highly active Fe₃₆Co₄₄ bimetallic nanoclusters catalysts for hydrolysis of ammonia borane: The first-principles study. *Chin. Chem. Lett.* **34**(2), 107261 (2023).
11. Zhang, L. *et al.* Experimental and DFT studies of flower-like Ni-doped Mo₂C on carbon fiber paper: A highly efficient and robust HER electrocatalyst modulated by Ni(NO₃)₂ concentration. *J. Adv. Ceram.* **11**(8), 1294–1306 (2022).
12. Li, D., Shen, X., Chen, L., Jiang, H. & Wang, J. The stability of covalently immobilization of TEMPO on the polymer surface through ionic liquid linkage: A comparative and model research. *De Gruyter* **15**(1), 39–44 (2015).

13. Nasrollahzadeh, M., Nezafat, Z., Bidgoli, N. S. S. & Shafiei, N. Use of tetrazoles in catalysis and energetic applications: Recent developments. *Mol. Catal.* **513**, 111788 (2021).
14. Swathi, S. *et al.* Cancer targeting potential of bioinspired chain like magnetite (Fe₃O₄) nanostructures. *Curr. Appl. Phys.* **20**(8), 982–987 (2020).
15. Chakraborty, S., Jähnichen, K., Komber, H., Basfar, A. A. & Voit, B. Synthesis of magnetic polystyrene nanoparticles using amphiphilic ionic liquid stabilized RAFT mediated miniemulsion polymerization. *Macromolecules* **47**(13), 4186–4198 (2014).
16. Çalışkan, M. & Baran, T. Design of a palladium nanocatalyst produced from Schiff base modified dialdehyde cellulose and its application in aryl halide cyanation and reduction of nitroarenes. *Cellulose* **29**(8), 4475–4493 (2022).
17. Omidi, M. H., Alibeygi, M., Piri, F. & Masoudifard, M. Polystyrene/magnetite nanocomposite synthesis and characterization: Investigation of magnetic and electrical properties for using as microelectromechanical systems (MEMS). *Mater. Sci. Poland* **35**(1), 105–110 (2017).
18. Krishnan, S. G., Pua, F.-L. & Zhang, F. A review of magnetic solid catalyst development for sustainable biodiesel production. *Biomass Bioenergy* **149**, 106099 (2021).
19. Roy, S. D., Das, K. C. & Dhar, S. S. Conventional to green synthesis of magnetic iron oxide nanoparticles; its application as catalyst, photocatalyst and toxicity: A short review. *Inorg. Chem. Commun.* **134**, 109050 (2021).
20. Kassaee, M. Z., Motamedi, E. & Majdi, M. Magnetic Fe₃O₄-graphene oxide/polystyrene: Fabrication and characterization of a promising nanocomposite. *Chem. Eng. J.* **172**(1), 540–549 (2011).
21. Chaudhari, M. A., Gujar, J. B., Kawade, D. S., Jogdand, N. R. & Shingare, M. S. Highly efficient and sustainable synthesis of dihydropyrano [2, 3-c] pyrazoles using polystyrene-supported *p*-toluenesulfonic acid as reusable catalyst. *Cogent Chem.* **1**(1), 1063830 (2015).
22. Takmil, N. F. *et al.* Hydrogen production by electrochemical reaction using waste zeolite boosted with titania and Au nanoparticles. *Inorg. Chem. Commun.* **133**, 108891 (2021).
23. Hajipour, A. R., Rezaei, F. & Khorsandi, Z. Pd/Cu-free Heck and Sonogashira cross-coupling reaction by Co nanoparticles immobilized on magnetic chitosan as reusable catalyst. *Green. Chem.* **19**(5), 1353–1361 (2017).
24. Khorsandi, Z., Borjian-Boroujeni, M., Yekani, R. & Varma, R. S. Carbon nanomaterials with chitosan: A winning combination for drug delivery systems. *J. Drug. Deliv. Sci. Technol.* **66**, 102847 (2021).
25. Khorsandi, Z., Metkazini, S. F. M., Heydari, A. & Varma, R. S. Visible light-driven direct synthesis of ketones from aldehydes via CH bond activation using NiCu nanoparticles adorned on carbon nano onions. *Mol. Catal.* **516**, 111987 (2021).
26. Mohammadi Metkazini, S. F., Khorsandi, Z., Heydari, A. & Varma, R. S. Sustainable visible light-driven Heck and Suzuki reactions using NiCu nanoparticles adorned on carbon nano-onions. *ACS Sustain. Chem. Eng.* **9**(42), 14061–14069 (2021).
27. Fathi Jasni, M. J. *et al.* Fabrication, characterization and application of laccase-nylon 6,6/Fe³⁺ composite nanofibrous membrane for 3,3′-dimethoxybenzidine detoxification. *Bioprocess Biosyst. Eng.* **40**(2), 191–200 (2017).
28. Khorsandi, Z., Hajipour, A. R., Sarfjoo, M. R. & Varma, R. S. A Pd/Cu-free magnetic cobalt catalyst for C–N cross coupling reactions: Synthesis of abemaciclib and fedratinib. *Green Chem.* **23**(14), 5222–5229 (2021).
29. Isacfranklin, M. *et al.* Single-phase Cr₂O₃ nanoparticles for biomedical applications. *Ceram. Int.* **46**(12), 19890–19895 (2020).
30. Wang, J. *et al.* MOF-derived NiFe₂O₄ nanoparticles on molybdenum disulfide: Magnetically reusable nanocatalyst for the reduction of nitroaromatics in aqueous media. *J. Ind. Eng. Chem.* **107**, 428–435 (2022).
31. Liu, Z., Fan, B., Zhao, J., Yang, B. & Zheng, X. Benzothiazole derivatives-based supramolecular assemblies as efficient corrosion inhibitors for copper in artificial seawater: Formation, interfacial release and protective mechanisms. *Corros. Sci.* **212**, 110957 (2023).
32. Nasrollahzadeh, M., Jaleh, B. & Jabbari, A. Synthesis, characterization and catalytic activity of graphene oxide/ZnO nanocomposites. *RSC Adv.* **4**(69), 36713–36720 (2014).
33. Baig, N., Kammakakam, I. & Falath, W. Nanomaterials: A review of synthesis methods, properties, recent progress, and challenges. *Mater. Adv.* **2**, 1821–1871 (2021).
34. Saravanan, M. *et al.* Green synthesis of anisotropic zinc oxide nanoparticles with antibacterial and cytofriendly properties. *Microb. Pathog.* **115**, 57–63 (2018).
35. Vidhya, M. S. *et al.* Anti-cancer applications of Zr Co, Ni-doped ZnO thin nanoplates. *Mater. Lett.* **283**, 128760 (2021).
36. Liu, W. *et al.* Treatment of Cr^VI-containing Mg(OH)₂ nanowaste. *Angew. Chem. Int. Ed.* **47**(30), 5619–5622 (2008).
37. Zhang, W. *et al.* Bioactive composite Janus nanofibrous membranes loading Ciprofloxacin and Astaxanthin for enhanced healing of full-thickness skin defect wounds. *Appl. Surf. Sci.* **610**, 155290 (2023).
38. Naveenraj, S. *et al.* A general microwave synthesis of metal (Ni, Cu, Zn) selenide nanoparticles and their competitive interaction with human serum albumin. *New J. Chem.* **42**, 5759–5766 (2018).
39. Zhang, K. *et al.* Facile synthesis of monodispersed Pd nanocatalysts decorated on graphene oxide for reduction of nitroaromatics in aqueous solution. *Res. Chem. Intermed.* **45**, 599–611 (2019).
40. Mirzaei, A., Esmkhani, M., Zallaghi, M., Nezafat, Z. & Javanshir, S. Biomedical and environmental applications of carrageenan-based hydrogels: A review. *J. Polym. Environ.* https://doi.org/10.1007/s10924-022-02726-5 (2022).
41. Majidi, S., Jaleh, B., Feizi Mohazzab, B., Eslamipanah, M. & Moradi, A. Wettability of graphene oxide/zinc oxide nanocomposite on aluminum surface switching by UV irradiation and low temperature annealing. *J. Inorg. Organomet. Polym. Mater.* **30**, 3073–3083 (2020).
42. Sonbol, H., Ameen, F., AlYahya, S., Almansob, A. & Alwakeel, S. *Padina boryana* mediated green synthesis of crystalline palladium nanoparticles as potential nanodrug against multidrug resistant bacteria and cancer cells. *Sci. Rep.* **11**, 5444 (2021).
43. Zhang, K. *et al.* Recent advances in the nanocatalyst-assisted NaBH₄ reduction of nitroaromatics in water. *ACS Omega* **4**(1), 483–495 (2019).
44. Baran, N. Y., Baran, T. & Çalışkan, M. Production of Pd nanoparticles embedded on micro-sized chitosan/graphitic carbon nitride hybrid spheres for treatment of environmental pollutants in aqueous medium. *Ceram. Int.* **47**(19), 27736–27747 (2021).
45. Mythili, R. *et al.* Utilization of market vegetable waste for silver nanoparticle synthesis and its antibacterial activity. *Mater. Lett.* **225**, 101–104 (2018).
46. Anis, S. M. *et al.* Decorated ZrO₂ by Au nanoparticles as a potential nanocatalyst for the reduction of organic dyes in water. *Inorg. Chem. Commun.* **141**, 109489 (2022).
47. Wang, Y., Wang, C., Wang, L., Wang, L. & Xiao, F.-S. Zeolite fixed metal nanoparticles: New perspective in catalysis. *Acc. Chem. Res.* **54**(11), 2579–2590 (2021).
48. Seitkalieva, M. M., Samoylenko, D. E., Lotsman, K. A., Rodygin, K. & S., Ananikov, V. P.,. Metal nanoparticles in ionic liquids: Synthesis and catalytic applications. *Coord. Chem. Rev.* **445**, 213982 (2021).
49. Sápi, A. *et al.* Metallic nanoparticles in heterogeneous catalysis. *Catal. Lett.* **151**, 2153–2175 (2021).
50. Zhang, K. *et al.* Pd modified prussian blue frameworks: Multiple electron transfer pathways for improving catalytic activity toward hydrogenation of nitroaromatics. *Mol. Catal.* **492**, 110967 (2020).
51. AlNadhari, S., Al-Enazi, N. M., Alshehrei, F. & Ameen, F. A review on biogenic synthesis of metal nanoparticles using marine algae and its applications. *Environ. Res.* **194**, 110672 (2021).
52. Zhao, Y. Co-precipitated Ni/Mn shell coated nano Cu-rich core structure: A phase-field study. *J. Mater. Res. Technol.* **21**, 546–560 (2022).

53. Alsamhary, K., Al-Enazi, N., Alshehri, W. A. & Ameen, F. Gold nanoparticles synthesised by flavonoid tricetin as a potential antibacterial nanomedicine to treat respiratory infections causing opportunistic bacterial pathogens. *Microb. Pathog.* **139**, 103928 (2020).

54. Ameen, F. *et al.* Fabrication of silver nanoparticles employing the cyanobacterium *Spirulina platensis* and its bactericidal effect against opportunistic nosocomial pathogens of the respiratory tract. *J. Mol. Struct.* **1217**, 128392 (2020).

55. Çalışkan, M. & Baran, T. Palladium nanoparticles embedded over chitosan/γMnO$_2$ composite hybrid microspheres as heterogeneous nanocatalyst for effective reduction of nitroarenes and organic dyes in water. *J. Organomet. Chem.* **963**, 122284 (2022).

56. Chokhachi Zadeh Moghadam, N. *et al.* Nickel oxide nanoparticles synthesis using plant extract and evaluation of their antibacterial effects on *Streptococcus mutans. Bioprocess Biosyst. Eng.* **45**(7), 1201–1210 (2022).

57. Roy, S., Senapati, K. K. & Phukan, P. Direct use of nanoparticles as a heterogeneous catalyst: Pd^0-doped CoFe$_2$O$_4$ magnetic nanoparticles for Sonogashira coupling reaction. *Res. Chem. Int.* **41**(8), 5753–5767 (2015).

58. Shokouhimehr, M. *et al.* Magnetically retrievable nanocomposite adorned with Pd nanocatalysts: Efficient reduction of nitroaromatics in aqueous media. *Green Chem.* **20**, 3809–3817 (2018).

59. Prasad, C., Sreenivasulu, K., Gangadhara, S. & Venkateswarlu, P. Bio inspired green synthesis of Ni/Fe$_3$O$_4$ magnetic nanoparticles using *Moringa oleifera* leaves extract: A magnetically recoverable catalyst for organic dye degradation in aqueous solution. *J. Alloys Comp.* **700**, 252–258 (2017).

60. Astruc, D. Transition-metal nanoparticles in catalysis: from historical background to the state-of-the art. Nanoparticles and Catalysis, Wiley-VCH Verlag GmbH & Co. KGaA, 1–48 (2008).

61. Faria, V. W. *et al.* Palladium nanoparticles supported in a polymeric membrane: an efficient phosphine-free "green" catalyst for Suzuki-Miyaura reactions in water. *RSC Adv.* **4**, 13446–13408 (2014).

62. Elazab, H. A., Radwan, M. A. & El-Idreesy, T. T. Facile microwave-assisted synthetic approach to palladium nanoparticles supported on copper oxide as an efficient catalyst for Heck and Sonogashira cross-coupling reactions. *Int. J. Nanosci.* **18**(05), 1850032 (2019).

63. Byun, S., Chung, J., Kwon, J. & Moon Kim, B. Mechanistic studies of magnetically recyclable Pd-Fe$_3$O$_4$ heterodimeric nanocrystal-catalyzed organic reactions. *Chem. Asian J.* **10**(4), 982–988 (2015).

64. Han, D., Zhang, Z., Bao, Z., Xing, H. & Ren, Q. Pd-Ni nanoparticles supported on titanium oxide as effective catalysts for Suzuki-Miyaura coupling reactions. *Front. Chem. Sci. Eng.* **12**, 24–31 (2018).

65. Heshmatpour, F., Abazari, R. & Balalaie, S. Preparation of monometallic (Pd, Ag) and bimetallic (Pd/Ag, Pd/Ni, Pd/Cu) nanoparticles via reversed micelles and their use in the Heck reaction. *Tetrahedron* **68**(14), 3001–3011 (2012).

66. Motahharifar, N., Nasrollahzadeh, M., Taheri-Kafrani, A., Varma, R. & S., Shokouhimehr, M.,. Magnetic chitosan-copper nanocomposite: A plant assembled catalyst for the synthesis of amino- and *N*-sulfonyl tetrazoles in eco-friendly media. *Carbohydr. Polym.* **232**, 115819 (2020).

67. Nasrollahzadeh, M., Motahharifar, N., Nezafat, Z. & Shokouhimehr, M. Copper(II) complex anchored on magnetic chitosan functionalized trichlorotriazine: An efficient heterogeneous catalyst for the synthesis of tetrazole derivatives. *Colloids Interface Sci. Commun.* **44**, 100471 (2021).

68. Sutradhar, P., Saha, M. & Maiti, D. Microwave synthesis of copper oxide nanoparticles using tea leaf and coffee powder extracts and its antibacterial activity. *J. Nanostruct. Chem.* **4**(1), 1–6 (2014).

69. Rout, L., Sen, T. K. & Punniyamurthy, T. Efficient CuO-nanoparticle-catalyzed C-S cross-coupling of thiols with iodobenzene. *Angew. Chem.* **46**, 5583–5589 (2007).

70. Yedurkar, S. M., Mauryal, C. B. & Mahanwar, P. A. A biological approach for the synthesis of copper oxide nanoparticles by *Ixora Coccinea* Leaf extract. *J. Mater. Environ. Sci.* **8**, 1173–1178 (2017).

71. Taghavi Fardood, S. & Ramazani, A. Green synthesis and characterization of copper oxide nanoparticles using coffee powder extract. *J. Nanostruct.* **6**(2), 167–171 (2016).

72. Sengupta, D. & Basu, B. An efficient heterogeneous catalyst (CuO@ARF) for on-water C-S coupling reaction: an application to the synthesis of phenothiazine structural scaffold. *Org. Med. Chem. Lett.* **4**, 17–27 (2014).

73. Bates, C. G., Saejueng, P., Doherty, M. Q. & Venkataraman, D. Copper-catalyzed synthesis of vinyl sulfides. *Org. Lett.* **6**(26), 5005–5008 (2004).

74. Sudhaik, A. *et al.* Copper sulfides based photocatalysts for degradation of environmental pollution hazards: A review on the recent catalyst design concepts and future perspectives. *Surf. Interfaces* **33**, 102182 (2022).

75. Cheng, L.-J. & Mankad, N. P. Copper-catalyzed carbonylative coupling of alkyl halides. *Acc. Chem. Res.* **54**(9), 2261–2274 (2021).

76. Zhao, C., Xi, M., Huo, J., He, C. & Fu, L. Computational design of BC$_3$N$_2$ based single atom catalyst for dramatic activation of inert CO$_2$ and CH$_4$ gases into CH$_3$COOH with ultralow CH$_4$ dissociation barrier. *Chin. Chem. Lett.* **34**, 107213 (2023).

77. Zhao, C., Xi, M., Huo, J. & He, C. B-Doped 2D-InSe as a bifunctional catalyst for CO$_2$/CH$_4$ separation under the regulation of an external electric field. *Phys. Chem. Chem. Phys.* **23**(40), 23219–23224 (2021).

78. Wang, X. *et al.* Electrochemically mediated decarboxylative acylation of *N*-nitrosoanilines with α-oxocarboxylic acids. *Chin. Chem. Lett.* **34**(2), 107537 (2023).

79. Wang, H. *et al.* Chiral 1,2-diaminocyclohexane-α-amino acid-derived amidphos/Ag(I)-catalyzed divergent enantioselective 1,3-dipolar cycloaddition of azomethine ylides. *Heterocycles* **104**, 123 (2022).

80. Liang, Y. *et al.* Benzene decomposition by non-thermal plasma: A detailed mechanism study by synchrotron radiation photoionization mass spectrometry and theoretical calculations. *J. Hazard. Mater.* **420**, 126584 (2021).

81. Ou, C., Pan, Y. & Tang, H. Electrochemically promoted N-heterocyclic carbene polymer-catalyzed cycloaddition of aldehyde with isocyanide acetate. *Sci. China Chem.* **65**(10), 1873–1878 (2022).

82. Zhao, S. *et al.* Recent advances on syngas conversion targeting light olefins. *Fuel* **321**, 124124 (2022).

83. Li, L. *et al.* Design and synthesis of tetrazole-based growth hormone secretagogue: The SAR studies of the O-benzyl serine side chain. *Bioorg. Med. Chem. Lett.* **18**, 1825–1829 (2008).

84. Upadhayaya, R. S. *et al.* Synthesis of novel substituted tetrazoles having antifungal activity. *Eur. J. Med. Chem.* **39**(7), 579–592 (2004).

85. Nasrollahzadeh, M. & Motahharifar, N. Synthesis of novel *N*-aryl-*N*-(1*H*-tetrazol-5-yl)benzenesulfonamides in water. *Appl. Organomet. Chem.* **34**(8), e5706 (2020).

Acknowledgements

Author contributions

M.N.: Supervision, Visualization, Validation, Writing—review and editing, Resources, Formal Analysis, N.M.: Methodology, Formal Analysis, Investigation, K.P.: Resources, Conceptualization, Investigation, Z.K.: Resources, Conceptualization, Investigation, Formal Analysis, T.B.: Conceptualization, Methodology, Writing: Original Draft, Formal Analysis, J.W.: Project administration, Fund Acquisition, Analysis, B.K.: Conceptualization,

Methodology, Investigation, Formal Analysis, H.A.K.: Conceptualization, Methodology, Investigation, Formal Analysis.

Competing interests

The authors declare no competing interests.

Additional information

Correspondence and requests for materials should be addressed to M.N.

Reprints and permissions information is available at www.nature.com/reprints.

Publisher's note Springer Nature remains neutral with regard to jurisdictional claims in published maps and institutional affiliations.